EVERGREEN - Joint Journal of Novel Carbon Resource Sciences & Green Asia Strategy, Vol. 13, Issue 03, pp. 1119-1135, September, 2026

Enhancing Viscoelastic Vibration Damping Efficiency in Natural Rubber Via Hybrid Nano – Filler: Advanced Finite Element Simulation and Experimental Integration

Adil Abed Nayeeif[1,*], Mayyadah S. Abed[2], Ahmed Ali Farhan Ogaili[1], Raed Naeem Hwayyin[3]

[1]Department of Mechanical Engineering, Mustansiriyah University, Baghdad, Iraq
[2]College of Materials Engineering, University of Technology, Baghdad, Iraq
[3]College of Electromechanical Engineering, University of Technology, Baghdad, Iraq

*Author to whom correspondence should be addressed:
E-mail: adilnayeeif@uomustansiriyah.edu.iq

(Received July 02, 2025; Revised June 03, 2026; Accepted August 11, 2026)

Abstract: In this study, three composite materials based on Natural Rubber are being investigated by the use of combined experimental and numerical methodology to analyze their vibration isolation behavior: Natural Rubber/Carbon Black (NR/CB), a mixture of Natural Rubber and Butadiene Rubber with Carbon Black (60% NR–40% BR/CB), and a nanocomposite of Natural Rubber/Silica and Carbon Black (NR-SiO 2/CB). Energy Dispersive Spectroscopy (EDS) and Scanning Electron Microscopy (SEM) were used to examine the materials in question in order to assess filler dispersion and microstructural interactions. Mechanical performance related to rotational excitation at 1000, 2000, and 3000 rpm was measured through tensile testing, compression set, rebound resilience, and vibration isolation tests. The damping behavior was investigated with the help of three basic parameters: logarithmic decrement (δ), damping ratio (ζ), and real damping coefficient (c). These parameters were measured on the basis of time-domain vibration data and confirmed on the basis of ANSYS Workbench 2019 mass-stiffness and finite element modeling. The OR-C=C-O-Si bridging nature of silica filler promoted the damping performance of the NR-SiO 2/CB nanocomposite in all the test conditions due to the augmentation of interfacial adhesion as well as constrained movement of molecules. The 60/40 NR/ BR/CB formulation exhibited a good overall balance of viscoelastic properties, while NR/CB was the least damping and most robust. Frequency-domain analysis and numerical simulations were used to point out the effect of material composition on vibrational response and modes of deformation, which were supported by experimental findings. The results highlight the importance of rubber formulation, type of filler, and dispersion to achieve the maximum energy dissipation performance. The FE analysis method combined with the experimental method is a reliable method to test the vibration isolation material under dynamic loading conditions.

Keywords: Blend; Dynamic Mechanical Analysis; Finite Element Analysis; Nanocomposite; Natural Rubber; Vibration Isolation

1. Introduction

Vibration isolation is a critical requirement in modern engineering uses in the automotive, aerospace, and industrial machinery sectors, in which uncontrolled vibrations may cause structural fatigue, noise pollution, and reduced operating efficiency[1,2]. Vibration analysis (VA) is a very important aspect of predictive maintenance in other sectors. It applies advanced signal processing techniques, such as time-frequency analysis and the Fast Fourier Transform (FFT), in order to enable early detection of defects in both rotating and non-rotating machines. Natural rubber (NR) and its composites have wide use in vibrating dampening due to their high energy dissipation capacity and viscoelastic properties[3]. Vibration isolation is achieved by mounting the structure on springs so that its natural frequency is lower than the imposed frequency[4]. illustrates the revolutionary potential of nanofiller-enhanced elastomers for vibration control applications by showing that alumina-zirconia (AlO_3-ZrO_2) nanoparticle reinforcement in natural rubber may increase storage

Cite: A. nayeeif et al., "Enhancing Viscoelastic Vibration Damping Efficiency in Natural Rubber Via Hybrid Nano - Filler: Advanced Finite Element Simulation and Experimental Integration". Evergreen, 13 (03) 1119-1135 (2026). https://doi.org/10.5109/7441040.

modulus by 260% while reducing vibration amplitude decay time by 25%[5]. By introducing rubber particles, which improve damping but decrease stiffness, this work aims to improve vibration damping in fiber/epoxy composites. Sonication was used to co-introduce silica nanoparticles in order to reduce this trade-off. Vacuum hand lay-up was used to create the laminates, and the half-power method and forced vibration were used for testing. Rubber particles considerably improved damping, particularly in off-axis laminates, according to micromechanical and finite element analyses, whereas silica nanoparticles assisted in maintaining rigidity. The damping improvement was limited with the 10 arrangements. All things considered, silica and rubber combine to improve damping while minimizing stiffness loss[6]. This study examines how the characteristics of styrene butadiene rubber (SBR) composites are affected by reinforcing fillers (AlO_3 and SiO_2) at different loading levels (0–25 pphr). Both fillers improved tensile strength, modulus, and elongation at break, according to mechanical tests, with silica exceeding alumina. 25 pphr of silica produced the maximum elongation (172%) and tensile strength (67 MPa). At the same loading, resilience, however, dropped to at least 65.59%. Additionally, silica-filled composites had the lowest wear rate (0.91 mm^3/mm) and the maximum hardness (85 IRHD). Physically, the amount of filler increased the resistance to swelling. Both fillers improved thermal conductivity, although alumina made a larger contribution. As filler loadings increased, so did specific gravity[7]. This study investigates how the physical characteristics of elastomeric compounds are affected when natural rubber (NR) and styrene-butadiene rubber (SBR) are blended together with different carbon black loadings (20–80 pphr). A total of twenty formulations with NR/SBR ratios of 0, 25, 50, 75, and 100 pphr were made. The findings indicated that while thermal conductivity and diffusivity rose with carbon black content, they fell with increasing NR content. Swelling was larger in water and decreased with both increased carbon black and higher NR content, as indicated by the mass change in water and oil. For all blends, specific gravity rose in direct proportion to carbon black dosage[8]. The performance of natural rubber/EPDM nanocomposites reinforced with graphene nanoplatelets (GNPs), made via melt compounding, in terms of vibrational damping is investigated in this work. The effects of chitosan-functionalization and GNP loading (1, 3, and 5 weight percent) were assessed. The findings demonstrate that GNPs considerably improve damping behavior, as seen by higher damping ratio and log decrement. However, this benefit is somewhat diminished by GNPs functionalized with chitosan. Storage modulus, loss modulus, and tan δ improvements were validated by dynamic mechanical analysis, and the reported improvements were supported by TEM analysis, which showed intercalated and exfoliated GNP structures. There is potential for these nanocomposites to be used as efficient vibration insulators[9]. By employing a bead mill to prepare silica/NR masterbatches, this study aims to improve silica dispersion in natural rubber (NR). The masterbatches' silica loadings, which varied from 10 to 30 phr, were contrasted with those of traditionally mixed compounds. Additionally assessed were the effects of the silane coupling agent Si-69. The results shown that cure retardation, which is frequently observed in traditional mixes, was removed by masterbatch manufacturing. Because of their improved dispersion, masterbatches containing >10 phr silica showed greater reinforcing even in the absence of Si-69. The masterbatch composites demonstrated similar abrasion resistance, rolling resistance, and heat build-up to their silane-filled conventional counterparts at silica levels below 30 phr. At all loadings, Si-69's damping characteristics were comparable to those of traditional composites[10]. The vibration-damping behavior of natural rubber composites, including waste tire rubber particles and precipitated silica of different sizes (100–250 µm, 550–700 µm, and 1000–1150 µm), is examined in this study. Two-roll milling was used to create the composites, and a hydraulic press was used to vulcanize them. The results showed that both direct and indirect testing techniques indicated that higher particle sizes greatly improved damping performance. Composites with larger particles showed increased energy absorption, according to differential scanning calorimetry (DSC), which helped to produce better damping properties. These results imply that massive waste tire rubber fillers work very well for applications involving vibration damping[11]. In order to improve vibration-damping capabilities, this study proposes a novel natural rubber (NR) nanocomposite that is reinforced with AlO_3–ZrO_2 nanoparticles (0–15 phr) and is patent pending (IPC India, File No. 1623/Mum/2014). SEM confirmed that the nanofillers were effectively dispersed and cross-linked during the material's synthesis, which took place under carefully regulated mixing and curing conditions. Both experimental and computational techniques were used to assess vibration-damping performance under impulsive excitation. In the Laplace domain, a simply supported beam model was created to examine dynamic behavior and frequency response. The findings demonstrated that the number of nanoparticles significantly influences the damping properties, such as amplitude attenuation, natural frequency, and settling time. The potential of this nanocomposite NR as a high-performance damping material was confirmed by the near alignment of theoretical and experimental results[12]. The vibration-damping capabilities of natural rubber (NR) composites containing precipitated silica (PSi) and fumed silica (FSi) are the main focus of this investigation. Well-dispersed silica/NR masterbatches were made using a latex-based technique. In addition to having greater viscosity, stiffness, and tear strength, FSi-filled NR composites also had higher rolling resistance and heat build-up, two characteristics that have an impact on damping. By increasing filler dispersion and lowering energy loss, the silane coupling agent Si-69 greatly improved damping-related parameters, particularly in FSi composites. These results demonstrate the promise of silica-filled NR, especially with FSi and Si-69, for sophisticated vibration-damping applications that demand mechanical stability and effective energy dissipation[13]. For improved vibration dampening, this study investigates the use of bamboo biochar (BBC) and recycled carbon black (RCB) as sustainable fillers in natural rubber (NR) composites. Three composites were created and tested for their mechanical, damping, and physical characteristics: NEAT NR, NR/30BBC, and NR/30RCB. As compared to Neat NR, the results indicated that NR/30RCB had the greatest gains in density, hardness, tensile strength, and tear strength. Tensile and tear strength improved by more than 550%. Notably, in free-layer damping testing, NR/30RCB obtained the highest damping ratio (ξ = 3), demonstrating its exceptional capacity to dissipate vibrational energy and promising for vibration isolation applications[14]. This work is aimed at studying the dynamic mechanical properties of the rubber composites with carbon nanotube (CNT) reinforcement. The authors were using CNTs as scattered nano-particles to enhance the behavior of viscoelastic. Dynamic mechanical analysis (DMA) was conducted at varying frequencies (0.01-50 Hz) as well as a temperature span of 20C to 100C with the help of a PerkinElmer PYRIS Diamond Dynamic Mechanical Analyzer. It has been found that the complex modulus of CNT-filled rubber is highly temperature and frequency dependent, which implies increased stiffness and energy loss. These improvements demonstrate CNT-reinforced rubber's promise for sophisticated vibration-damping and dynamic loading applications[15]. Small-angle X-ray scattering and rheological investigation revealed high connections between microstructure and damping behavior in silica nanocomposites based on NR, demonstrating their ability to restore mechanical integrity post-processing[16]. Incorporating stearic acid-modified diatomaceous earth and carbon nanotubes into NR matrices resulted in better filler-rubber interaction and damping capability[17]. Graphene-based hybrid fillers for rubber composites emphasize their effective function in energy dissipation under dynamic stress[18]. studied thermal and mechanical damping in carbon-based NR nanocomposites, stressing the impact of filler conductivity and polymer viscoelasticity[19]. Finite element and dynamic modeling were used to examine magnetorheological elastomer composites with NR-based matrix, which confirmed the usefulness of FE approaches for damping predictions[20]. performed ABAQUS-based FE simulations of hyperelastic composite dampers, validating models under sinusoidal loads and confirming hysteretic damping behavior compatible with tests[21]. We developed and verified waveguide-based constitutive models for pre-compressed NR isolators, demonstrating good prediction of dynamic stiffness and damping under fatigue conditions[22]. investigated the nonlinear dynamic behavior of rubber-layer roller bearings (RLRBs), demonstrating their damping performance under seismic stimulation, validated using FE simulations[23]. Conducted combined numerical-experimental research on zinc oxide nanoparticle-reinforced CR/NR composites, utilizing hyper elastic finite-element models that matched experimental damping to within 5% error[24]. used FE modeling to estimate damping properties of rubber-geopolymer concrete cantilever structures, confirming increases in energy dissipation with greater rubber content[25]. This research investigates the use of nanotechnology as an alternative sustainable filler to traditional fillers in the belt division and discusses the scarce studies involving the use of nanosilica in the belt division. The investigation focuses on the effects of nanosilica on the dynamic mechanical properties of Natural Rubber (NR) and Styrene-Butadiene Rubber (SBR) blends. The rheological, mechanical and morphological properties of the fabricated nanocomposites were investigated thoroughly and compared to the existing carbon black filled control samples. The experimental results show that the service life of the nanosilica-based belts is considerably superior to that of regular belts, which results in a 15% increase[26]. This may indicate the potential use of nanofillers in creating more durable rubber products for specific operating conditions that are more environmentally friendly. The effectiveness of surface modified precipitated silica (SiO_2) as an reinforcement of natural rubber (NR) nanocomposites in the home industry vibration isolation application is critically reviewed. Investigating a loading range of 0–20 phr, the research is able to establish a precise structure–property correlation between silica dispersion and viscoelastic response. The analytical data indicated that the critical point for optimal performance are 10 phr with tensile strength 19.6 MPa and tan $¥delta$ of 0.18. This is a 2X higher damping capacity than neat NR and results in a vibration transmissibility decrease of 63–71% at operational frequencies (15–25 Hz). Moreover, the 10 phr loading also increased the thermal stability for 18°C. The results in this study show that these reinforced silica materials are a superior solution to standard rubber based elasto-materials for use in attenuation systems for domestic appliances[27]. In view of the above, this study critically focuses on the synergistic effect of surface modified carbon black/nanosilica hybrid systems for the reinforcement of IIR. This work compares the basic change in viscoelastic properties and cross-link density that occurs as a result of the coupling agent treatments, as opposed to traditional additive studies. The

Cite: A. nayeeif et al., "Enhancing Viscoelastic Vibration Damping Efficiency in Natural Rubber Via Hybrid Nano - Filler: Advanced Finite Element Simulation and Experimental Integration". Evergreen, 13 (03) 1119-1135 (2026). https://doi.org/10.5109/7441040.

results indicate not only an incremental improvement, but a transformative approach to increasing Delta Torque by 13% and optimizing glass transition temperature (Tg). Glass fiber-reinforced epoxy composites are known to be widely used to make structures, but the stiffness and the thermal properties of traditional fillers with rubber matrix limits their use in extreme conditions. This paper attempts to overcome these shortcomings by investigating the multifunctional reinforcement capacity of carbon nanotubes (CNTs) in composite tubes using state-of-the-art Finite Element Method (FEM) simulations. The study replaces the traditional homogeneous modeling approach with a nanostructured reinforcement analysis and defines the critical threshold value of the CNT content for the structural integrity/weight balance at 1%, which leads to an increase of 22% in tensile strength. In addition, the correlation between the CNT content and buckling resistance highlights a basic improvement in load distribution mechanisms. This computational validation provides a solid framework for predicting the synergistic thermal and mechanical improvements in nanohybrid tubes which is more applicable than the traditional fiber-reinforced tubes[29].

Although the natural rubber is widely-used in the industrial damping, the synergistic interaction between the hybrid nano-fillers and rubber matrices under high-frequency rotational excitation is still not fully understood. Hence, in this study, the aim is to overcome this gap by taking a dual experimental and numerical approach. In addition, the study aims to establish a comprehensive model based on the Finite Element Analysis (FEA) method that accurately predicts the dynamic transmissibility, which is validated thoroughly with actual acceleration data. This research uses SEM and EDS to correlate the performance of the passive vibration isolator at macro-mechanical level with the dispersion of the microstructures, and thus a detailed understanding of how to make the passive vibration isolator perform well for specific domestic and industrial applications.

The principal objectives of this study are: (i) to fabricate and characterize three NR-based composite formulations with different filler systems; (ii) to evaluate their vibration damping performance experimentally under rotational excitation at 1000, 2000, and 3000 RPM using time-domain and frequency-domain analysis; (iii) to determine key damping parameters including logarithmic decrement (δ), damping ratio (ζ), and real damping coefficient (c); and (iv) to validate experimental findings through three-dimensional finite element modal and transient analyses using ANSYS Workbench. The integrated experimental–numerical framework developed here provides a robust methodology for evaluating and selecting rubber-based vibration isolation materials for industrial dynamic applications

2. Experimental Work

2.1. Materials and processes

Using high cis-butadiene rubber (BRcis) and SMR 20 natural rubber as basic polymers, rubber compounds were made by ASTM D3182-16[30]. Precipitated silica (20–40 nm) and carbon black (N330) were employed as partial and primary fillers, respectively. Zinc oxide, castor oil, and paraffin wax were used as processing aids, and sulfur, TMQ, CBS, and CTP were part of the curing system. Table 1 lists the formulations in detail[31].

To create masterbatch sheets, rubber compounds were combined in a two-roll mill using a constant mixing procedure for five minutes at room temperature with a 1.5 mm nip gap. NR/CB, 60NR-40BRcis/CB, and NR/CB/SiO_2 nanocomposites were the three formulations that were made. Using a hot press, vulcanization was performed for 45 minutes at 155°C and 13 MPa. Babylon Tires Company, Diwaniyah Tires Factory, and the Universities of Technology and Baghdad in Iraq were the sites of processing, molding, curing, and testing.

2.2. SEM and EDS characterization

A scanning electron microscope (SEM) and energy-dispersive spectroscopy (EDS) were used to analyze the nano silica powder and rubber samples, enabling investigation of their homogeneity and topography. The VEGA 3 TESCAN SEM and ZEISS equipment were operated at acceleration voltages of 5 and 20 kV, with varying magnifications from 1x to 250,000x.

2.3. Testing of vibration damping

Damping is the ability to absorb energy. There are two techniques for determining damping properties: the first one is a direct method (measuring energy dissipation directly), such as rebound resilience. The second one is an indirect method (measuring amplitude and frequency,

Table 1: Natural Rubber-Based Composites and Nanocomposites: Formulations (phr)

Material	#1 pphr	#2 pphr	#3 pphr
NR (SMR20)	100	60	100
BR_{cis}	-	40	0
Zinc oxide	5.5	5.5	5.5
(TMQ)	1.5	1.5	1.5
Paraffin wax	0.5	0.5	0.5
Castor oil	5	5	5
Carbon black (N330)	25	50	50
Precipitated silica (SiO_2)	25	0	0
(CBS)	1.5	1.5	1.5
Sulphur	2.3	2.3	2.3
CTP.100	0.15	0.15	0.15

Cite: A. nayeeif et al., "Enhancing Viscoelastic Vibration Damping Efficiency in Natural Rubber Via Hybrid Nano - Filler: Advanced Finite Element Simulation and Experimental Integration". Evergreen, 13 (03) 1119-1135 (2026). https://doi.org/10.5109/7441040.

which are related to energy dissipation, dynamic modulus, and compression set percentage). This work is based on the indirect method.

The experimental setup and rubber specimen shapes used to assess vibration isolation and rebound resilience are shown in Figure 1. A mechanical vibration testing machine that simulates dynamic loading by controlled harmonic stimulation is the primary piece of equipment, as seen in Figure 1a. To evaluate damping performance, a rotating unbalance motor is installed within a vibration isolation chamber. To test their ability to attenuate vibrations, rubber specimens were positioned between the load platform and the vibrating base. A disc-shaped rubber sample (40 mm in diameter and 4 mm in thickness) manufactured following established testing procedures serves as the standard specimen, as seen in Figure 1-b. Also included is a molded rubber sheet with many labeled samples (1, 2, 3). The three distinct rubber formulations, NR/CB, NR-BR/CB, and NR/CB/SiO_2 nanocomposite, are shown in Figure 1-c. A rebound pendulum is used for the resilience test. This test is carried out according to ASTM D 1054, with the specimens (40 mm dia. 4 mm thick), using a Wallace Dunlop Tripsometer.

Figure 2-a, A specially made mold for creating rubber vibration isolators in the shape of cylinders. During the vulcanization process, the manually clamped steel mold allows for consistent pressure and heat application. This equipment was used to precisely shape and cure rubber specimens at the Diwaniyah Tire Factory in Iraq. Rubber vibration isolators with steel rods inserted were fabricated and labeled 1 through 3 based on the various compound formulations (1) NR/CB, (2) 60NR-40BR/CB, and (3) NR/CB/SiO_2. Figure 2-b. These samples were ready for further isolation testing, including vibration and mechanical testing.

Compressive deformation of elastomeric materials is measured where a cylindrical rubber specimen is tested on a standard compression set tester, as illustrated in Figure 3a. The complete system is shown on the left side, which comprises the vertically aligned compression set up comprising of guide rods and mechanical loading arrangement. A helical spring ensures that loads are applied consistently with each other. Metallic spacers and load-distribution plates are used to maintain the specimen under constant strain, temperature, and time, which is provided in the ASTM D395 Method B, which is displayed in the middle-magnified image. The configuration guarantees reproducible force and axial alignment for precise measurement of permanent deformation. The specimen is shown in Figure 3b prior to testing, with dimensions chosen to ensure a constant contact area and satisfy conventional testing standards (29 mm diameter, 12.5 mm height).

(a) (b)

Fig. 1: Wallace Dunlop Tripsometer and samples in molds

(a) (b)

Fig. 2: Manufacturing and Characterization of Rubber Vibration Isolator Samples

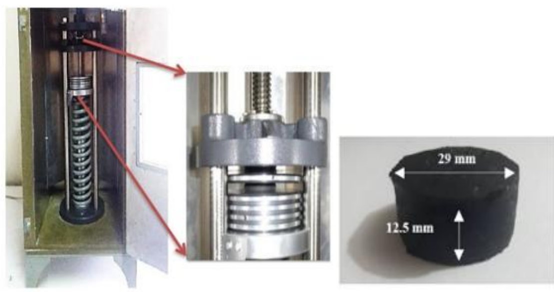

(a) (b)

Fig. 3: Tester for Compression Sets and Rubber Sample

Figure 4a displays a set of rubber specimens in the shape of dumbbells that have been prepared for tensile testing. They are labeled and meet ASTM D412 (Type C) criteria for assessing the tensile characteristics of vulcanized rubber and thermoplastic elastomers. The specimen measurements shown in the schematic in Figure 4b are 115 mm in total length, 33 mm in gauge length, 6 mm in reduced width, and 3 mm in thickness. A 14 mm fillet radius connects the narrow and broad portions. During testing, localized deformation and consistent stress distribution are guaranteed by the gauge section.

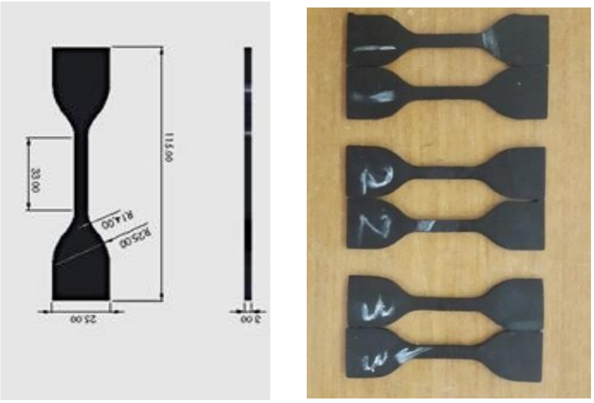

(a) (b)

Fig. 4: Typical Rubber Tensile Specimens

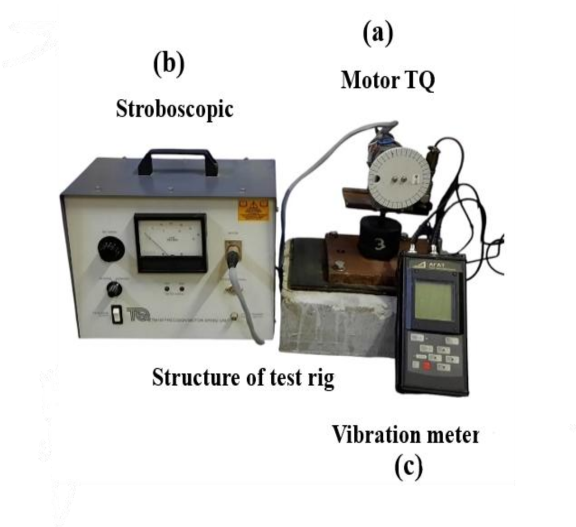

Fig. 5: Set up for measuring rotational vibration using a motor speed control unit and a vibration analyzer. (a) Motor (b) Stereoscopic (c) Vibration meter

Al-Mustansiriyah University's Mechanical Engineering Department allows precise motor speed control in increments of 250 RPM from 250 to 3000 RPM. The stroboscopic disk, which is fixed to the motor shaft and marked in degrees, allows for visual synchronization with the stroboscope. This allows for accurate shaft rotation observation and the identification of torsional vibrations Figure 5b. Sensors on the motor or the structure foundation are linked to the digital AFAT device, the vibration meter Figure 5c. It displays signals in both the time and frequency domains and detects the frequency and amplitude of vibrations. At every speed setting, vibration data is gathered in order to assess structural integrity and resonance.

The specimen is a cylinder (75 mm diameter, 59 mm length). The measured parameter is natural frequency. A tensile test was also executed to obtain the axial stiffness (K) of the sample from the Young modulus. This test was done according to ASTM D 412, as shown in Figure 2-b.

3. Results and Discussion

The morphology and elemental composition of the silica nanoparticles produced were analyzed by the use of Scanning Electron Microscopy (SEM) and Energy Dispersive X-ray Spectroscopy (EDS). Though the total distribution remained the same, the image of SEM at various magnifications showed mostly spherical particles with smooth surfaces and a tendency to form agglomerations. Their nanoscale size and outlined boundaries were demonstrated by high magnification (251.79 KX).

Based on the expected composition of SiO 2, EDS showed that silicon (Si) and oxygen (O) are the main components. In the case of Si and O, the atomic percentages were approximately 42.1% and 54.9% respectively and the trace element of sulfur (S) most probably came about due to the remains of synthesis. Such results confirm that high-purity silica nanoparticles of a spheroidal shape and an average diameter of 20-60 nm were effectively synthesized. The prevailing Si and O peaks can be observed in the SEM images and EDS spectra[7,8] as presented in Figure 6.

SEM of natural rubber/carbon black (NR/CB) composites at magnifications of 10.00 KX and 50.01 KX are shown in Figure 7. The micrographs reveal a rough granular surface that has an observable agglomeration of carbon black particles. At a lower magnification, the composite appears packed tightly implying that the carbon black is well spread within the rubber matrix. Localized agglomeration is observed in higher magnification, meaning that there is partial clustering and thus it might influence electrical or mechanical performance. NR composites' folded and layered structure facilitates robust filler–matrix interactions. These physical characteristics draw attention to carbon black's reinforcing function in the NR matrix.

Figure 8 illustrates SEM of the 60NR/40BR (cis)/CB composite at 10.00 KX and 50.01 KX showing magnifications, which highlight the carbon black (CB) dispersion and surface morphology in the NR/BR composite. On lower magnification, a coarse, irregular surface with close-spaced features is observed. The microstructure has interconnected spherical and semi-spherical particles that signify strong filler-matrix bonding as well as 5efficient CB networking that can enhance the modulus and tensile strength. At low agglomeration and uniformly dispersed CB particles, the surface appears more defined in higher magnification, which means that there is good compatibility between the rubber phases and CB. To maximize the reinforcing impact of carbon black, this consistent dispersion facilitates effective load distribution and stress transfer. Additionally, the morphology indicates that BR helps to increase composite homogeneity and dispersion.

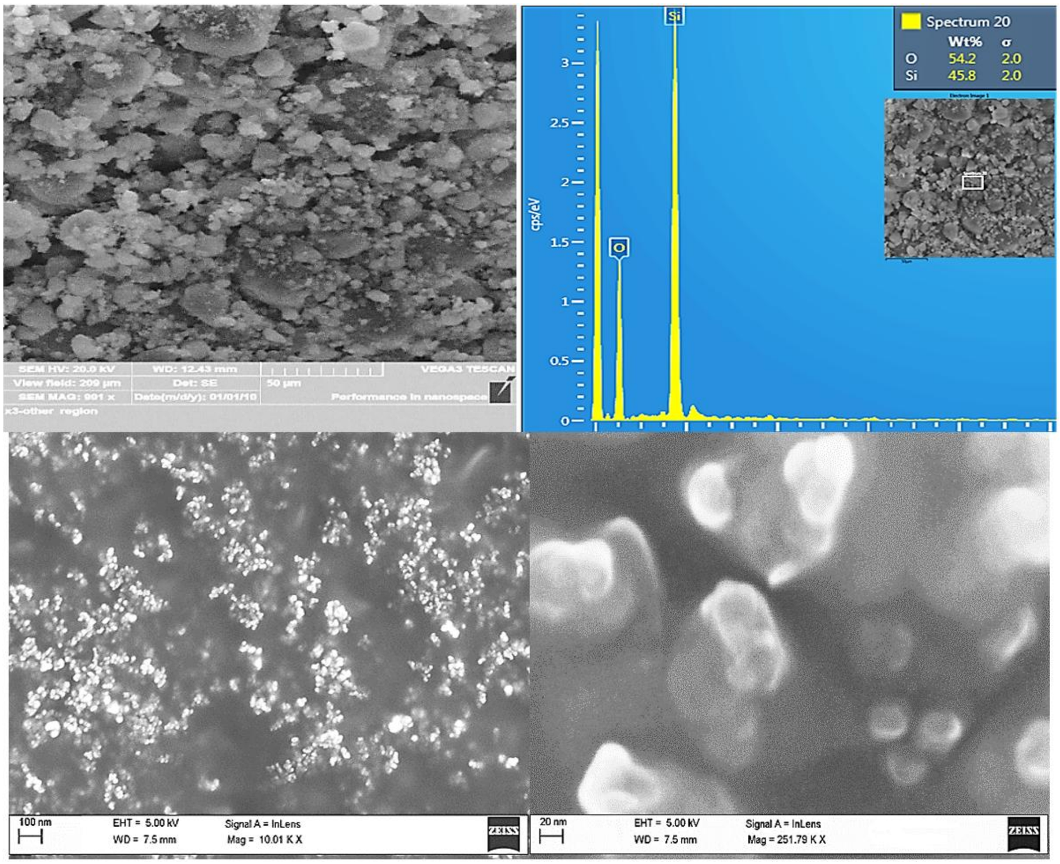

Fig. 6: SEM and EDS analysis of silica nanoparticles

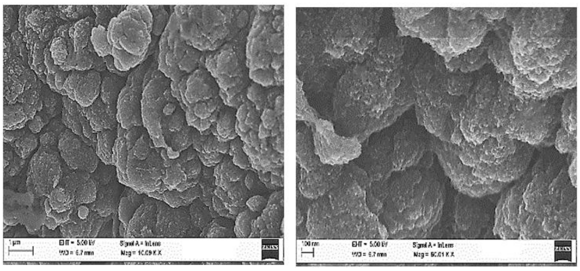

Fig. 7: SEM images of samples NR/CB

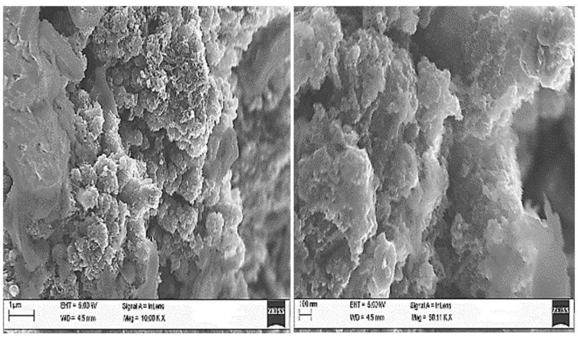

Fig. 8: SEM samples 60NR-40BRcis/CB blend

SEM micrographs of the NR/CB/SiO_2 nanocomposite at 10.00 KX and 50.11 KX are displayed in Figure 9, which depicts the morphology and dispersion of silica (SiO_2) and carbon black (CB) within the natural rubber (NR) matrix. course, uneven surface with aggregated structures is seen at lower magnification, suggesting partial filler agglomeration that is probably caused by surface energy differences or inadequate mixing. However, indications of network creation point to enhanced conductivity and mechanical reinforcement. With areas of both uniform dispersion and localized aggregation, CB and SiO_2 nanoparticles are easier to discern at higher magnification. SiO_2 is particularly noticeable because of its hydrophilic nature in contrast to the hydrophobic NR matrix. Compatibilizers or surface treatment could improve dispersion. Notwithstanding some clustering, CB and SiO_2 work in concert to improve conductivity and tensile strength, while SiO_2 increases thermal stability and abrasion resistance. Strong filler–matrix interaction and uniform dispersion are prerequisites for optimal performance.

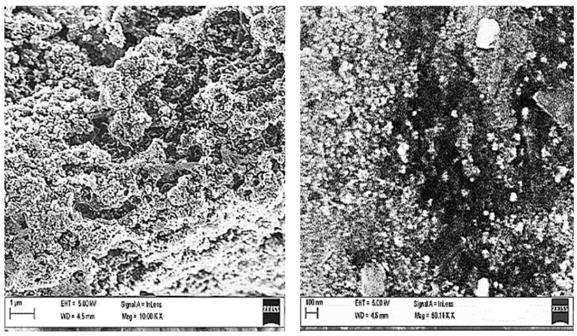

Fig. 9: SEM of samples NR/CB/SiO_2 nanocomposite

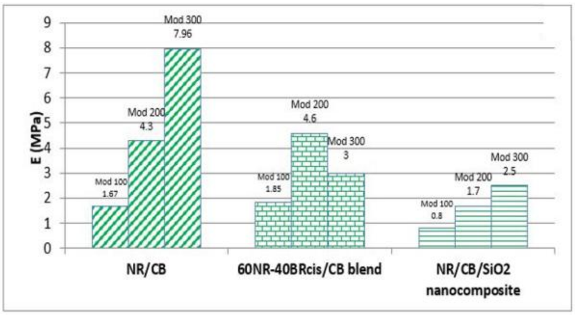

(a)

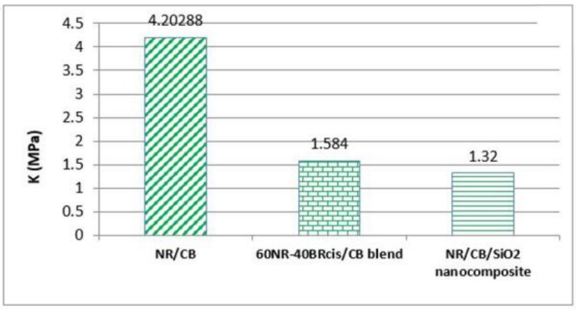

(b)

Fig. 10: Young modulus and axial stiffness

modulus and stiffness, followed by 60NR-40BRcis/CB blend and then NR/CB/SiO_2 nanocomposite. That gives a rough indication of damping properties. The materials that have the highest modulus and stiffness give the lowest damping properties at all, as shown in Figure10.

Figure 11 (a, b, c) displays the prepared samples' damping characteristics, which include the damping ratio, compression set, and rebound resilience, respectively. The NR/CB composite showed the lowest damping ratio, minimal compression set, and the highest rebound resilience. The NR/CB/SiO_2 nanocomposite, on the other hand, demonstrated the highest compression set, the highest damping ratio, and the lowest resilience (greater damping). The dampening properties of the 60NR-40BRcis/CB combination were middling. Material type and microstructure have a strong influence on damping behavior, as evidenced by previous SEM results[32,33]. NR/CB's capacity to recover under dynamic loads is facilitated by its cave-like shape. As cavity size decreases, this resilience decreases in the 60NR-40BRcis/CB blend and even more in the NR/CB/SiO_2 nanocomposite[34]. This pattern is a result of the rubber chains' limited mobility, which raises energy dissipation and improves damping[35].

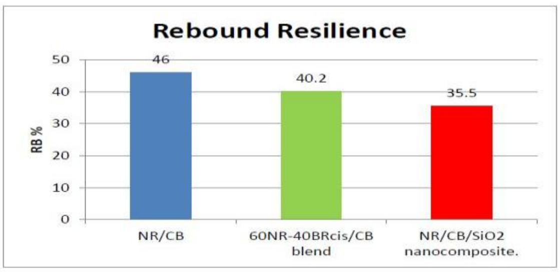

(a)

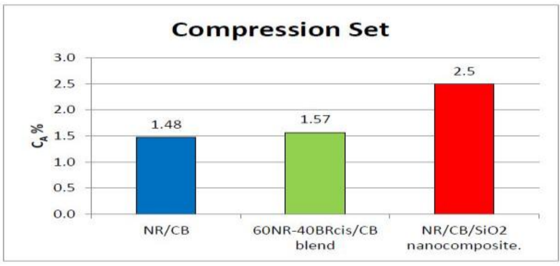

(b)

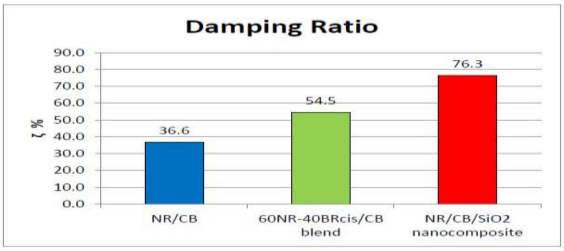

(c)

Fig. 11: Damping properties of samples, where a) rebound resilience, b) compression set, and c) Damping ratios of samples NR/CB; 60NR-40BRcis/CB blend; and NR/CB/SiO_2

4. Vibrations Experimental Results

Three composite samples in Table 1, vibration responses were examined in order to determine how well they dampened under controlled excitation. The base of each sample was fastened to a concrete foundation and positioned vertically to remove the effects of external vibrations in Figure 5. At the sample base, a steel plate and concrete were separated by a vibration-isolating layer to reduce noise and guarantee precise measurements. A thick steel plate held an external vibration motor at the top, limiting movement to the longitudinal axis. Using a stroboscope controller, the motor speed was adjusted at 250 RPM increments from 250 to 3000 RPM in order to produce steady dynamic excitation. A vibration meter recorded time and frequency domain data, while an accelerometer placed at the top of each sample recorded transmitted vibration signals[36]. The complete speed range was measured, but the main speeds 1000, 2000, and 3000 RPM were the subject of in-depth analysis, which highlighted frequency spectra and time-domain waveforms. To compare the sample vibration behavior and damping efficiency, the peak amplitudes at each speed are considered.

4.1. Time Domain

Figures 12, 13, and 14 demonstrate the amplitude, as a function of time, with vibration response of three rubber composites, NR/CB, 60NR-40BRcis/CB, and NR/CB/SiO_2 nanocomposite under rotational speed (1000, 2000, and 3000 RPM) load. These charts indicate the damping of the materials as the intensity of excitation increases.

Figure 12 shows the vibrations at 1000 RPM with NR/CB as the lowest, followed by 60NR-40BRcis/CB and NR/CB/SiO_2. These small amplitudes exhibit sufficient damping under low excitation. NR/CB reacts better due to its higher rigidity (Modulus 300 = 7.96 MPa). Either a lack of interfacial bonding or an optimum silica dispersion leads to the higher amplitude of NR/CB/SiO 2 at reduced excitation. These findings are consistent with recent studies that show that low dynamic damping capacity is caused by low silica dispersion in the NR matrices[37].

More noticeable changes in vibration behavior are indicated in Figure 13. NR/CB has a high growth of amplitude up to 5 m, meaning that the material is either near the resonance conditions or that its damping efficiency is being surpassed at this degree of excitation. NR/CB/SiO_2 has a greater amplitude but smaller than NR/CB. It is important to note that the amplitude of 60NR-40BRcis/CB is low, which suggests that it is well-damped. This performance might be explained by the fact that it contains BRcis, which enhances the dissipation energy as a result of the more flexible shape of molecules. The lower modulus and stiffness provided in this sample under higher strain level (Modulus 300 = 3 MPa) indicate a movement and energy absorption on the inside.

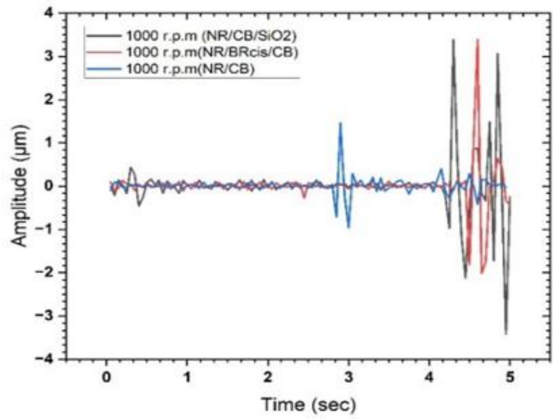

Fig. 12: Time-domain vibration response of three rubber composite samples at 1000 r.p.m

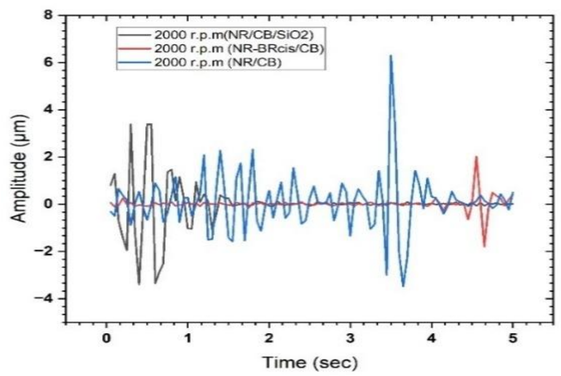

Fig. 13: Time-domain vibration response of three rubber composite samples at 2000 r.p.m

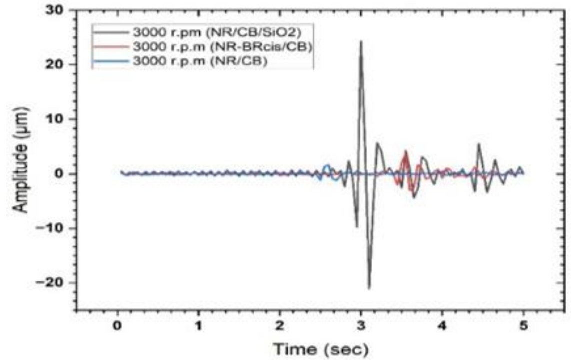

Fig. 14: Time-domain vibration response of three rubber composite samples at 3000 r.p.m

Figure 14, the NR/CB/SiO_2 sample shows a significant rise in amplitude, reaching ±20 μm, indicating resonance or inadequate damping performance at this speed. This could be attributed to interfacial slippage or poor compatibility between silica nanoparticles and the rubber matrix, resulting in localized stress concentrations. Meanwhile, NR/CB exhibits moderate amplitude oscillations, but 60NR-40BRcis/CB continues to display good damping behavior with the lowest amplitude response. This supports the previous discovery that the BRcis component improves damping performance, most likely through molecular mobility and viscoelastic energy dissipation.

4.2. Frequency Domain

This paper investigates the vibration behavior of composite materials of rubber-based materials at different rotational speeds to determine their dynamic behavior. The natural rubber compounds analyzed are reinforcing with different types of reinforcing materials, including carbon black (CB), high cis-butadiene rubber (BRcis) and silica. The goal is to understand how the composition of the material influences the study[38] am SiO2 -cis -CB-NR /CB amplitude and damping characteristics through the analysis of the frequency-domain vibration amplitude spectrum of three different composite materials: NR/CB/SiO2, NR-BRcis/CB, and NR/CB.

Cumulative frequency-domain vibration amplitude spectra of three composite types NR/CB/SiO_2, NR-BRcis/CB and NR/CB are shown in Figure 15, 16 and 17, respectively. This provides a comparison of their dynamic responses. This study offers a scientific and engineering-based interpretation of how composite formulation impacts vibrational performance, which is important for applications requiring rotating machinery and structural vibration control.

In Figure 15, when the sample is excited at 1000 r.p.m., the NR/CB sample has the smallest amplitude, meaning that it has more damping effects at lower frequencies. This is because the dispersion and interaction between the rubber matrix and carbon black particles are effective which enhances energy dissipating capacity through internal friction. The NR/CB/SiO_2 sample shows the highest

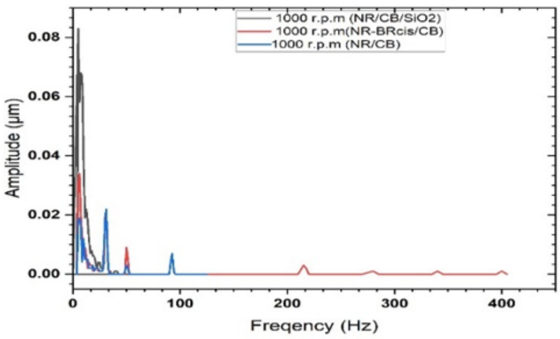

Fig. 15: Vibration Amplitude Spectrum at 1000 r.p.m. for Different Rubber-Based Composites

amplitude, suggesting that the sample is not very damping. The most likely explanation is poor separation of silica particles and the rubber. This causes slippage and energy retention instead of energy dissipation. The composite of NR-BRcis has an intermediate response, and these flexible chains together with carbon black particles contribute to the composite in a balanced way[28].

Figure 16, At 2000 r.p.m., the amplitude increases for all samples, especially for NR/CB/SiO_2, which achieves a substantially greater peak. This means the system is approaching resonance conditions or that the damping capacity is being exceeded at this excitation level. The SiO_2-filled composite absorbs vibrational energy less efficiently, underscoring the need for filler-matrix compatibility. On the other hand, NR-BRcis/CB maintains a reasonably controlled amplitude, which can be attributed to the improved viscoelastic nature of BRcis rubber, allowing for more internal movement and energy absorption. NR/CB continues to perform admirably, with only a minor rise in amplitude, demonstrating its effective damping action.

Figure 17. At 3000 r.p.m., all samples exhibit a drop in amplitude, with NR/CB/SiO_2 still showing the strongest response. The observed reduction may be due to the system running beyond its resonance frequency, where inertial and damping forces prevail. Additionally, centrifugal stiffening effects at high speeds may lower vibration amplitude. The NR-BRcis/CB sample continues to exhibit steady damping characteristics. In contrast, NR/CB has the

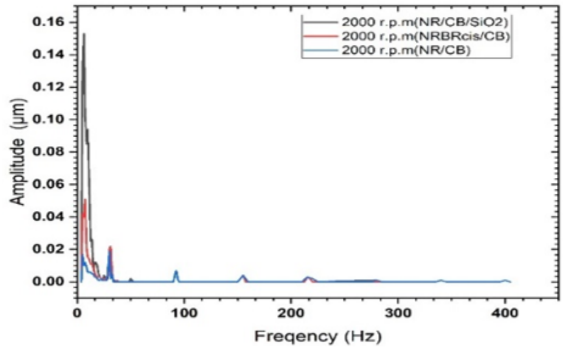

Fig. 16: Vibration Amplitude Spectrum at 2000 r.p.m. for Different Rubber-Based Composites

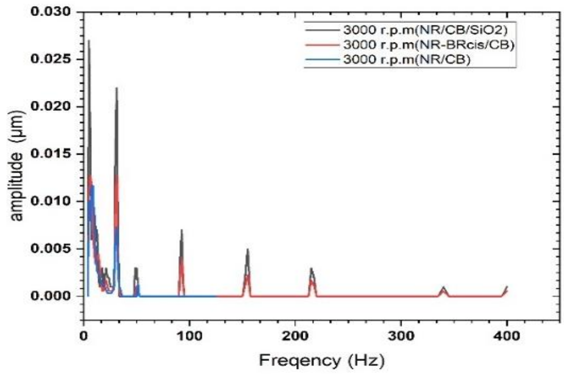

Fig. 17: Vibration Amplitude Spectrum at 3000 r.p.m. for Different Rubber-Based Composites

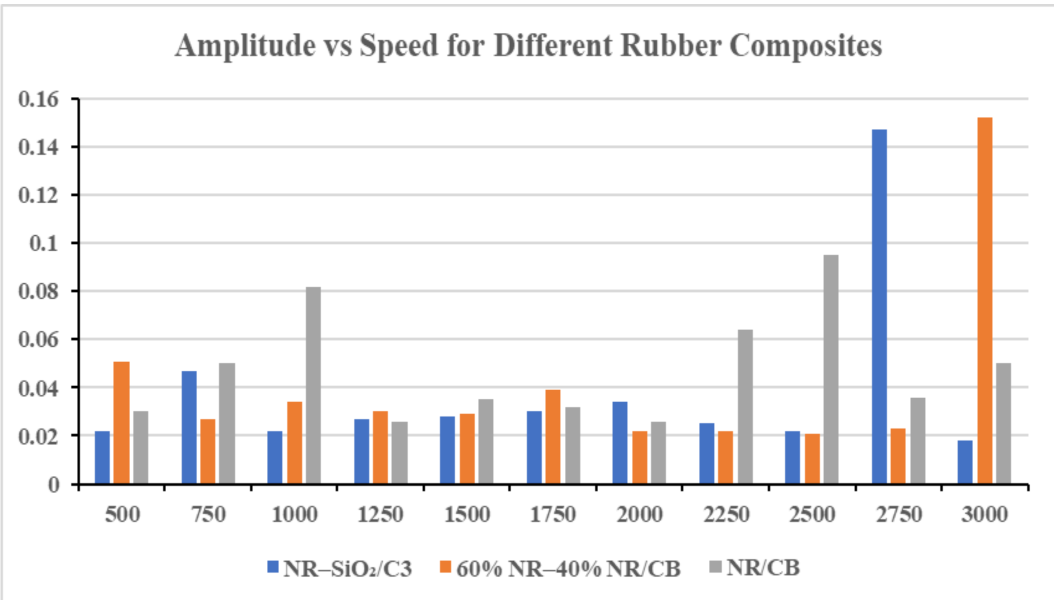

Fig. 18: Maximum amplitude with frequency for each sample (FFT)

lowest and most consistent amplitude, highlighting its applicability for high-speed applications needing vibration control.

Figure 18 illustrates substantial differences in vibrational behavior among the three rubber composites at varying rotating speeds. The NR/CB sample had the most stable performance, with continuously low to moderate amplitudes and a peak of 0.095 µm at 2500 r.p.m. This indicates efficient damping due to strong filler-matrix interaction. The NR-BRcis/CB sample exhibits a significant amplitude increase at 3000 r.p.m. (0.153 µm), indicating resonance or reduced damping at high speeds. The NR/SiO_2 sample shows fluctuating behavior, with a noticeable peak at 2750 r.p.m. (0.147 µm), possibly due to lower interfacial interaction between silica and the rubber matrix. Overall, NR/CB has the best damping properties, making it ideal for applications with variable-speed vibrations.

5. Vibrations Numerical Results

The numerical method based on the Finite Element Method (FEM) was used with ANSYS 2019 R3 software. A three-dimensional computational model of the cylindrical specimen was created using the dimensions shown in Figure 2b, which have a diameter of 75 mm and a length of 50 mm. These dimensions were applied to the three specimens shown in Table 1. The meshing approach used SOLID185 elements, which are appropriate for 3D structural research. A structured hexahedral mesh was created to ensure accuracy and numerical convergence. The finished mesh has 84,232 nodes and 19,703 elements, as shown in Figure 19. The material properties assigned to each model were derived from experimental measurements: the elastic modulus (Young's modulus) was obtained from tensile test data, the density was calculated from specimen mass and geometry, and Poisson's ratio was set to 0.49 for all rubber formulations, consistent with the nearly incompressible nature of vulcanized rubber. A mesh sensitivity study was conducted by comparing the fundamental natural frequency at three mesh densities (coarse: ~10,000 elements, medium: 19,703 elements, and fine: ~38,000 elements). The medium mesh yielded results within 0.8% of the fine mesh, confirming convergence at the selected density.

Figure 20 depicts the application of a fixed support to one face of the cylindrical specimen to imitate the experimental boundary conditions. This constraint limits all translational degrees of freedom on the chosen surface, assuring mechanical stability throughout the numerical study. The setup represents the actual testing settings used in the experimental technique.

Modal analysis was performed using ANSYS Mechanical APDL (2019 R3), applying structural physics with fixed support on one face of each cylindrical specimen to simulate experimental conditions. The three specimens, each with distinct mechanical properties in Table 1, were analyzed to extract natural frequencies and mode shapes. Simulation results in Figure 21 show that NR/CB deforms most (171.25 mm at 232.75 Hz), reflecting its high elasticity and limited stiffness increase from carbon black. The 60 NR-40 BR composite exhibits slightly reduced deformation (164.02 mm at 234.70 Hz), as BRcis enhances stiffness and resilience. The NR/CB/SiO_2 model displays the lowest deformation (155.67 mm at 146.41 Hz), due to additional damping and constraints from silica. These findings demonstrate that both material composition and external damping factors significantly influence vibrational response, with hybrid formulations and added damping effectively reducing structural deformation.

The robust correlation between the experimental displacement data and the Finite Element Method (FEM) predictions underscores the efficacy of the developed viscoelastic model. The observed reduction in vibration transmissibility, particularly in the NR-SiO_2/CB nanocomposites, is not merely a numerical outcome but a reflection of complex micro-mechanical phenomena. Physicochemically, the integration of nanosilica promotes a dense filler network and enhances the Polymer-Filler interaction, which restricts the mobility of the elastomer chains. This restriction facilitates a higher rate of energy dissipation through internal molecular friction, thereby increasing the loss factor (δ).

Furthermore, as highlighted in recent literature regarding surface treatment effects on NR/BR composites[39)], the synergy between carbon black and silica fillers creates a dual-reinforcement mechanism. This mechanism optimizes the stress distribution within the rubber matrix, leading to the significant attenuation of peak accelerations observed at 2000 and 3000 rpm. The numerical results confirm that the hybrid filler system effectively transforms kinetic energy into thermal energy at the interfacial regions, a critical factor in enhancing the operational life of passive isolators in high-frequency environments.

The maximum total deformation of three rubber-based composites, NR/CB, 60% NR -40% BR/CB, and NR -SiO 2/CB in six vibrational modes is presented in Figure 22. The highest deformation is attained at Mode 5 in all the specimens, which is their resonant frequencies. Since natural rubber is highly elastic and carbon black does not reinforce to a very large extent, allowing the material to move much more dynamically, NR/CB is the most prone to deformation (171.25 mm at 232.75 Hz). The 60% NR-40 percent BR/CB compound has a slightly reduced deformation (164.02 mm at 234.7 Hz) through the addition of butadiene rubber, which adds rigidity and resilience and reduces susceptibility to vibrations. NR SiO 2/ CB has the lowest deformation (155.67 mm at 146.41 Hz), which indicates that silica decreases dynamic response by enhancing stiffness and damping capacity.

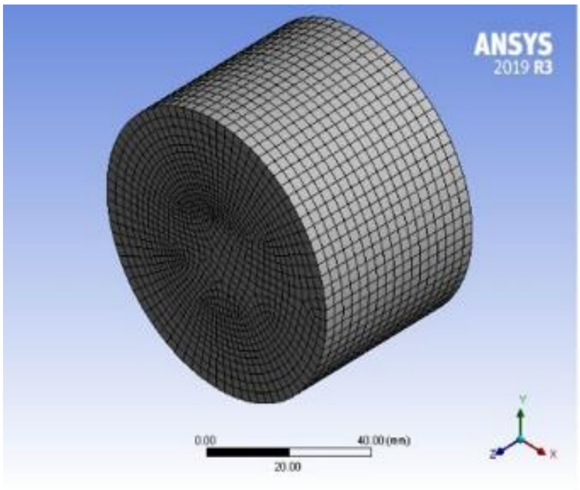

Fig. 19: Finite element mesh of a cylindrical specimen

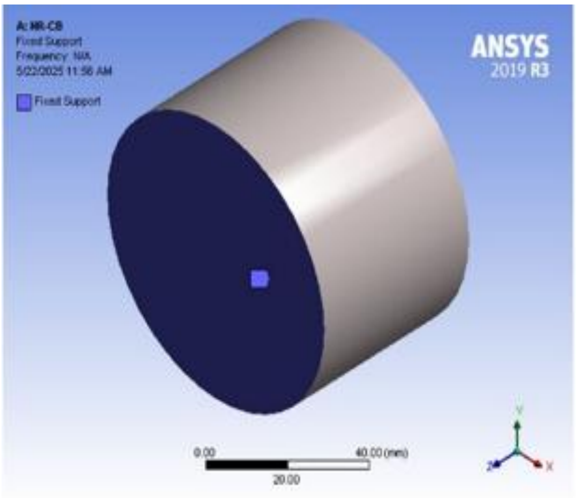

Fig. 20: A fixed support boundary condition is applied to the cylindrical specimen

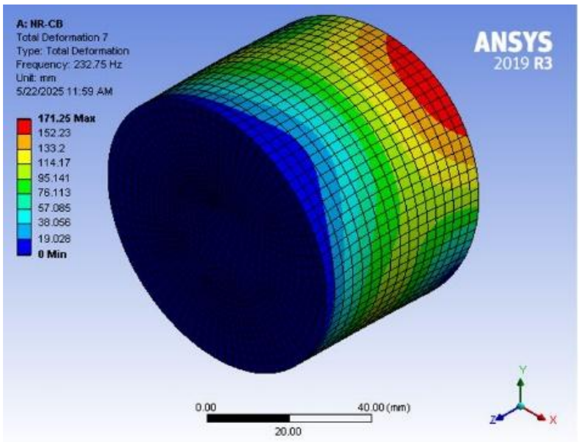

(a)

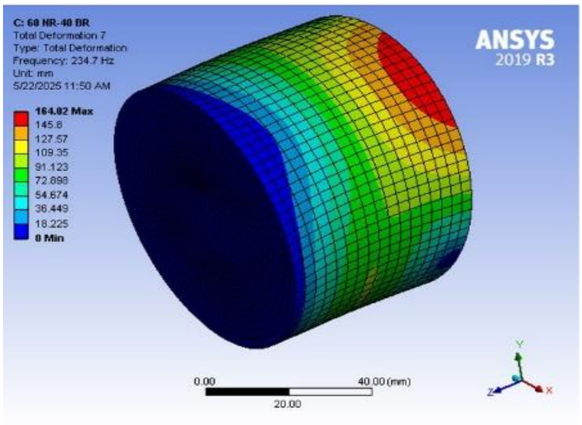

(b)

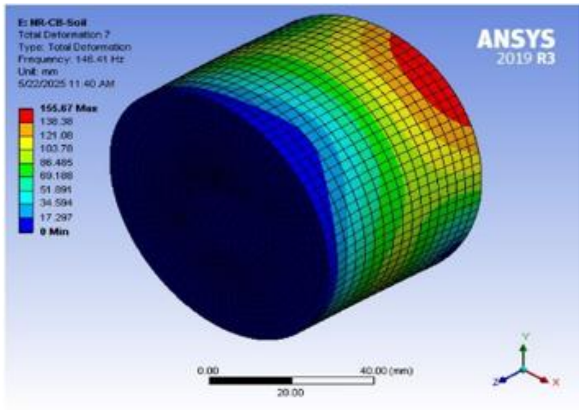

(c)

Fig. 21: Total Deformation at Mode 7 for Various Rubber-Based Composites Under Vibrational Loading; (a) NR/CB (b) 60%NR-40% BR/CB (c) NR-SiO_2/CB

The lowered resonance frequency of this specimen is also an indication of altered mass stiffness properties. These results highlight the significance of the filler type in modifying the dynamic deformation and improving the system in regard to vibration resistance, particularly in silica-based systems.

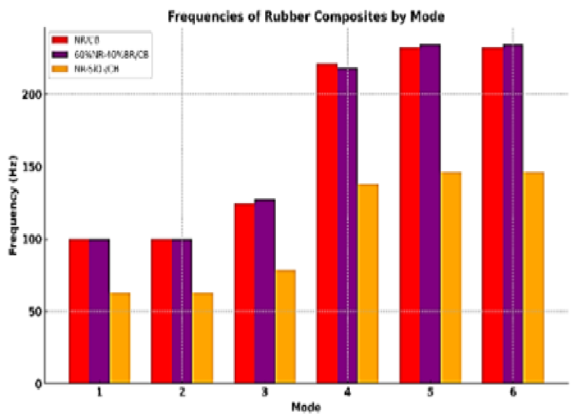

Fig. 22: Maximal Deformation Values for Higher Vibration Modes for Rubber-Based Composites

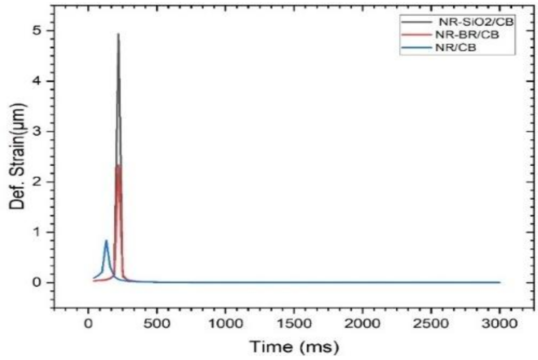

Fig. 23: Transient Deformation Response of Rubber Composites

Figure 23 shows the deformation strain response over time of three rubber composite materials: NR/CB, NR-BR/CB (60%NR-40%BR), and NR-SiO_2/CB. The Figure shows that NR-SiO_2/CB has the highest initial strain response, followed by NR-BR/CB. NR/CB has the lowest deformation peak. NR-SiO_2/CB and NR-BR/CB exhibit the fastest strain decrease, indicating rapid vibrational energy dissipation. In contrast, NR/CB decays more slowly, allowing residual vibrations to last longer. This behavior can be linked to the internal structure and filler type of each composite. Silica in NR-SiO_2/CB increases interfacial contact and inhibits molecular mobility, leading to improved stiffness and damping efficiency. Similarly, adding BR to NR-BR/CB enhances energy dissipation through greater viscoelastic response. Meanwhile, NR/CB is a simpler composition with less filler reinforcement, resulting in more elastic behavior and poorer energy dissipation capacity. The results show that NR-SiO_2/CB and NR-BR/CB are more effective for vibration suppression and structural damping. As a result, they are more suited to dynamic industrial applications that require quick vibration decline[40]

6. Damping Results

The damping behavior is important in the vibration analysis and characterisation of materials in determining the suitability of a material in dynamic applications. Composites made of rubber are most commonly used in vibration isolator systems due to the viscoelastic nature of rubber. The present study is aimed at checking the damping properties of three different rubber composite specimens subjected to rotating excitations[41]at different speeds. The experiment was done on 3 materials: NR/CB, 60%NR-40%BR/CB, and NR-SiO_2 /CB, and the rotating speed was 1000, 2000, and 3000 RPM. Three damping parameters were calculated, including logarithmic decrement, the damping ratio, and the real damping coefficient (c)[42].

The damping behaviour of rubber composite materials of 1000, 2000, and 3000 RPM was realized by using a homogeneous method to assess the damping behaviour of the materials in rubber composite: 1000NR/CB, 60%NR-40%BR/CB, and NR-SiO_2/CB. In each case of testing condition three paramount damping measures were identified sequentially: the logarithmic decrement, damping ratio, and the real damping coefficient.

Figure 24. Comparison between the time domain vibration signal acquired in each example. The first two consecutive peak amplitudes are identified by using this signal. The logarithmic decrement is then calculated using these data and it is the rate at which the amplitude of the vibration reduces between cycles.

This is then divided by a constant factor which is the oscillatory nature of the system resulting in the damping ratio. Damping ratio is a normalized measure of the dissipation of energy, which shows the degree to which the system is near to a critical damping state.

The important damping coefficient is then determined using the mass and the stiffness of each specimen. This coefficient represents the hypothetical value at which the vibrations come to a stop. Lastly, dividing the damping ratio with the critical damping value gives the actual damping coefficient that measures the actual ability of the system to dissipate vibrational energy.

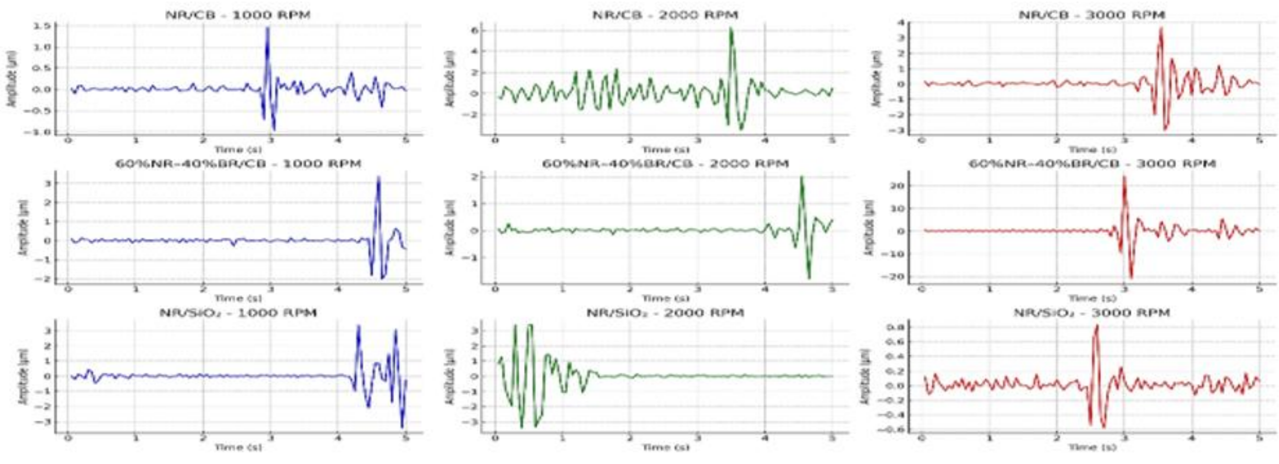

Fig. 24: Signals of Vibration for all Samples with different speeds

Table 2 presents the quantitative damping metrics—logarithmic decrement (δ), damping ratio (ζ), and real damping coefficient (c)—for the three composite specimens tested at 1000, 2000, and 3000 RPM. The physical parameters differ as follows: NR/CB (mass = 0.2098 kg, stiffness = 600 N/m), 60%NR–40%BR/CB (0.2325 kg, 700 N/m), and NR–SiO_2/CB (0.2552 kg, 800 N/m). These differences in mass and stiffness directly govern the critical damping coefficient and hence the magnitude of the real damping coefficient for each specimen. NR–SiO_2/CB consistently achieved the highest damping values at all rotational speeds. At 3000 RPM, its logarithmic decrement reached δ = 0.599, damping ratio ζ = 0.095, and real damping coefficient c = 12.15 Ns/m. These represent improvements of approximately 46%, 46%, and 53%, respectively, over the NR/CB baseline at the same speed (δ = 0.410, ζ = 0.065, c = 7.92 Ns/m).

It is believed that the high performance of NRSiO 2/CB is due to the presence of ORC=C=O=Si bridging structure that develops as a result of the silane coupling mechanism and which boosts the interfacial adhesion and limits the mobility of rubber chains, hence, raising the internal friction and energy dissipation of the interface between fillers and the matrix. This mechanism is in line with the results of Prasertsri and Rattanasom, who established that silane-functionalized silica enhances the damping-related parameters significantly by increasing dispersion and decreasing energy-loss mechanisms. The 60%NR-40%BR/CB mixture had a mid-range performance with 503, 80, and 11.53 Ns/m at 3000 RPM-23, 23, and 46 times better than NR/CB, respectively. The BRcis component reduces the glass transition temperature and the presence of a more flexible molecular backbone that facilitates an increase in viscoelastic energy dissipation during dynamic loading. This agrees with the findings on GNP-reinforced NR/EPDM blends in which the damping behavior is enhanced by the introduction of flexible rubber phases. The monotonic trend of δ, zone, and c with rotational speed between 1000 and 3000 RPM was observed in all three composites, which is an indicator of the frequency-dependent viscoelastic nature of rubber. The accelerating c can be attributed to processes that are dependent upon strain rate, 87300 energy loss, such as filler rubber chain disentanglement and interface excitation between filler and matrix at high excitation frequencies. Generally, NR 5 SiO_2/CB is the formula of choice in high-speed industrial use, including engine mounts, 5 execute machinery isolation pads, and dynamic sealing elements. The 60 percent of the NR-40 percent of the BR/CB blend is a viable balance ratio of flexible couplings and suspension components, whereas NR/CB is still applicable in the case of applications with less severity, where recovering is prioritized.

Table 2: Damping parameters (δ, ζ, c) for all rubber composite samples at various rotational speeds

Sample	Ω (RPM)	(δ)	(ζ)	(c) [Ns/m]
NR/CB	1000	0.245	0.039	4.73
	2000	0.316	0.050	6.06
	3000	0.410	0.065	7.92
60%NR–40%BR/CB	1000	0.298	0.047	6.80
	2000	0.355	0.057	8.20
	3000	0.503	0.080	11.53
NR–SiO_2/CB	1000	0.430	0.068	8.71
	2000	0.510	0.081	10.35
	3000	0.599	0.095	12.15

7. Conclusions

a) NR -SiO 2/CB recorded the highest total vibration damping between the three composites. It had the maximum logarithmic decrement (δ = 0.599), damping ratio (ζ = 0.095) as well as real damping coefficient (c = 12.15 Ns /m), which were an improvement of 46 and 46 and 53, respectively, over the base NR/CB composite. The syneristic effect of silica and carbon black fillers is enabled by the interfacial bonding of OR-C=C-O-Si bonds to inhibit the movement of the molecular chains and increase the dissipation of energy due to friction within themselves.

b) The 60 percent NR40 percent BR/CB mix provided 60 percent damping, which was intermediate and of practical use, in terms of 60 percent of the NR40 percent BR/CB mix at 3000 RPM, with 8 values of 0.503, 0.080, and 11.53 Ns/m. The BRcis phase flexible molecular structure reduces the glass transition temperature and facilitates viscoelastic energy dissipation to give a balanced combination of performance in terms of damping efficiency and elasticity to fit flexible couplings, dynamic gaskets, and suspension bushings.

c) NR/CB was the worst damping (δ = 0.410, 0.065 ζ, 7.92 Ns/m 3000 RPM); however, with the highest rebound resilience and the lowest compression set due to its simpler filler system and higher elastic recovery capacity. It is still applicable to general-purpose isolation applications in which robustness and elastic recovery are more important than energy dissipation efficiency.

d) The trends of the experimental trends were confirmed with the FEM modal analysis (ANSYS Workbench 2019 R3): the natural frequency (146.41 Hz) and the total deformation (155.67 mm at Mode 7) of NR 3SiO2/CB were the lowest, which revealed that silica reinforcement could cause the changes in the dynamic response to lower frequencies and reduce structural deformation. The near consensus between FEM simulations and experimental findings justifies the numerical method of numerical modeling of rubber composite vibration isolators.

e) The natural rubber is naturally well adapted to vibration isolation because it is highly viscoelastic fatigue life, tensile strength, and adhesion to metal surfaces. These findings of this research indicate that damping performance of NR is controllably adjusted by the choice of filler and the blending of polymer. The addition of silica nanoparticles (NR/CB/SiO 2) resulted in the most significant increase in the damping values, whereas mixing with BRcis (60NR -40BRcis/CB) provided a convenient tradeoff between damping and flexibility. The experimental-numerical methodology that has been integrated in this work offers a confirmed and repeatable framework of the analysis of evaluating and ranking rubber-based vibration isolation materials within industrial dynamic loading conditions.

Acknowledgments

The author of this study would like to express their heartfelt gratitude to all of their colleagues in the Department of Mechanical Engineering, particularly those in the College of Engineering at Mustansiriyah University (https://www.uomustansiriyah.edu.iq/), who have contributed to the success and growth of this work.

References

1) M. S. Abed, A. A. Nayeeif, H. Abdulkhalik. "Comparative study of transverse vibration and mechanical properties of aluminium, Al 7020 alloy, and MWCNTs reinforced aluminium nanocomposites." Int. J. Nanoelectron. Mater. 13 (3), 509–522 (2020).
2) T. Chu, T. Nguyen, H. Yoo, J. Wang. "A review of vibration analysis and its applications." Heliyon 10(3), e26282 (2024). doi:10.1016/j.heliyon.2024.e26282.
3) M. F. Omar, F. Ali, M. S. Jami, A. S. Azmi, F. Ahmad, M. Z. Marzuki, S. K. Muniyandi, Z. Zainudin, M. P. Kim. "A comprehensive review of natural rubber composites: Properties, compounding aspects, and renewable practices with natural fibre reinforcement." J. Renew. Mater. 13(3), 497–518 (2025). doi:10.32604/jrm.2024.057248 .
4) Y. Fukahori. "Use of natural rubber (NR) for vibration isolation and earthquake protection of structures." In: S. Kohjiya, Y. Ikeda (Eds.), Chemistry, Manufacture and Applications of Natural Rubber, 371–381. Woodhead Publishing (2014). doi:10.1533/9780857096913.2.371.
5) R. Muhammad, B. Kumar, A. Chaskar. "Modal analysis of nanoparticles reinforced natural rubber." IOSR J. Mech. Civ. Eng. 11(3), 45–52 (2014), doi: 10.9790/1684-11344552.
6) C.-Y. Huang, J.-L. Tsai. "Characterizing vibration damping response of composite laminates containing silica nanoparticles and rubber particles." J. Compos. Mater. 48(0), 1–14 (2014). doi:10.1177/0021998314521257 .
7) J. K. Oleiwi, M. S. Hamza, M. Sh. Abed. "Improving the properties of the tire tread by adding SiO_2 and Al_2O_3 to SBR rubber." Int. J. Appl. Eng. Res. 5(9), 1637–1652 (2010).
8) J. K. Oleiwi, M. S. Hamza, N. A. Nassir. "A study of the effect of carbon black powder on the physical properties of SBR/NR blends used in passenger tire treads." Eng. Technol. J. 29(5), 856–870 (2011), doi:10.5281/zenodo.3838695.
9) N. Mohamad, M. H. N. Talib, A. Z. R. M. Shukor, A. R. Othman, R. Zahari. "Vibrational damping behaviors of graphene nanoplatelets reinforced NR/EPDM nanocomposites." J. Mech. Eng. Sci. 11(4), 3274–3287 (2017). doi:10.15282/jmes.11.4.2017.28.0294.
10) S. Prasertsri, N. Rattanasom. "Mechanical and damping properties of silica/natural rubber composites prepared from latex system." Polym. Test. 30(5), 515–526 (2011). doi:10.1016/j.polymertesting.2011.04.001.
11) V. Chandran, L. Nagarajan, M. R. Thomas. "Evaluation of vibration-damping behavior of different sizes of waste tyre rubber in natural rubber composites." J. Compos. Mater. 0(0), 1–9 (2016). doi:10.1177/0021998166671219.
12) R. Muhammad, B. Kumar. "Natural rubber-based hybrid nanocomposite vibration dampers." Int. J. Adv. Res. 5(6), 1314–1323 (2017). doi:10.21474/IJAR01/4542.
13) S. Prasertsri, N. Rattanasom. "Fumed and precipitated silica reinforced natural rubber composites prepared from latex system: Mechanical and dynamic properties." Polym. Test. 31(5), 593–605 (2012). doi:10.1016/j.polymertesting.2012.03.003.
14) Sunali, J. Mago, A. Negi, S. Fatima. "Vibration damping properties of natural rubber composites developed with waste carbonaceous fillers." J. Acoust. Soc. India 51(1), 8–15 (2024).
15) D. Bakosová. "Dynamic mechanical analysis of rubber mixtures filled with carbon nanotubes." Manuf. Technol. 18(3), 345–351 (2018) ,doi: 10.21062/ujep/103.2018/a/1213-2489/MT/18/3/345.
16) K. Boonsomwong, A.-C. Genix, E. Chauveau, J.-M. Fromental, P. Dieudonné-George, C. Sirisinha, and J. Oberdisse, Rejuvenating the structure and rheological properties of silica nanocomposites based on natural rubber, Polymer, 202 (2020), 122646.

Doi:10.1016/j.polymer.2020.122646.

17) M. N. Alam, V. Kumar, H.-S. Jung, S.-S. Park. "Fabrication of high-performance natural rubber composites with enhanced filler–rubber interactions by stearic acid-modified diatomaceous earth and carbon nanotubes." Polymers 15, 3612 (2023), doi: 10.3390/polym15173612.
18) J. Wang, S. Li, L. Yang, B. Liu, S. Xie, R. Qi, Y. Zhan, H. Xia. "Graphene-based hybrid fillers for rubber composites." Molecules 29, 1009 (2024) , doi: 10.3390/molecules29051009**.**
19) F. Shahamatifard, D. Rodrigue, F. Mighri. "Thermal and mechanical properties of carbon-based rubber nanocomposites: A review." Plast. Rubber Compos. 52, 483–505 (2023), doi:10.1080/14658011.2023.2231286.
20) E. Yarali, M. A. Farajzadeh, R. Noroozi, A. Dabbagh, M. J. Khoshgoftar, M. J. Mirzaali. "Magnetorheological elastomer composites: Modeling and dynamic finite element analysis." Compos. Struct. (2020), doi:10.1016/j.compstruct.2020.112881.
21) T. W. Teh, C. G. Tan, and M. Z. Jumaat, "Feasibility Evaluation of Novel High-Damping Rubbers as Energy-Dissipation Material under Axial Dynamic Load for Damper Devices," *Buildings*, vol. 12, no. 11, p. 1917, (2022), doi: 10.3390/buildings12111917
22) L. Kari, S. Oberst, X. Gong. "Using waveguides to model the dynamic stiffness of pre-compressed natural rubber vibration isolators." Polymers 13, 472 (2021) , doi:10.3390/polym13111703.
23) N. Menga, F. Bottiglione, G. Carbone. "The nonlinear dynamic behavior of a rubber-layer roller bearing (RLRB) for vibration isolation." ArXiv Prepr. (2024), doi: arXiv:2401.16880.
24) E. K. Njim, F. A. Hadi, M. N. Hamzah. "Numerical and experimental investigation of nano-zinc oxide's effect on mechanical properties of CR/NR composites." ResearchGate Prepr. (2024), doi: 10.15330/pcss.25.1.14-25**.**
25) G. C., D. Z., W. X., J. S. "Modeling of damping characteristics of rubber geopolymer concrete based on finite element simulation." Buildings 12, 2142 (2023) , doi: 10.3390/buildings12122142.
26) T. R. A. S. Mohan, T. Kalalvendhan, and A. M. Adhil, "Determination of Dynamic Mechanical Properties on Addition of Carbon Black-Nanosilica Hybrid Fillers in NR-SBR Blends with Special Reference to Power Transmission Belt Applications," International Journal of Polymer Science, vol. 2024, Art. no. 3101938, pp. 1–13, Apr. 2024. doi: 10.1155/2024/3101938.
27) R. Hore, P. Sreenivasan, A. Kumar, S. Giri, P. Banerji, and S. Chattopadhyay, "Development of an eco-friendly vibration isolator using slag and SiC-reinforced natural rubber composite for automotive application: An approach towards circular economy," *Construction and Building Materials*, vol. 509, Art. no. 145222, 2026, doi: 10.1016/j.conbuildmat.2026.145222.
28) F. Jaberi Mofrad, A. Ahmadpour, and S. Ostad Movahed, "The effect of modified carbon black and nano silica, individually and in combination, on the curing, mechanical, and dynamical properties of butyl rubber (IIR)," Polymers and Polymer Composites, vol. 32, pp. 1–15, Mar. 2024. doi: 10.1177/09673911241238758.
29) A. S. Hussein, M. J. Jweeg, and A. A. Al-Humairi, "Finite Element Analysis of the Effects of Nanoparticle Reinforcement on the Physical and Mechanical Properties of Composite Tubes," International Journal on Advanced Science, Engineering and Information Technology, vol. 15, no. 1, pp. 245–255, Feb. 2025. doi: 10.18517/ijaseit.15.1.21408.
30) ASTM International. "Standard practice for rubber materials, equipment, and procedures for mixing standard compounds and preparing standard vulcanized sheets." ASTM D3182-07 2012 (2012). doi:10.1520/D3182-07R12.
31) A. A. Nayeeif, M. S. Abed, H. Abdulkhalik. "Morphology, rheology, and mechanical properties of NR, NR/BR, and NR nanocomposite." J. Eng. Sci. Technol. 17(5), 3512–3525 (2022).
32) D. D. L. Chung. "Review: Materials for vibration damping." J. Mater. Sci. 36(24), 5733–5737 (2001). doi:10.1023/A:1012999616049.
33) J. E. Mark, B. Erman, F. R. Eirich (Eds.). The science and technology of rubber (4th ed.). Elsevier (2013). doi:10.1016/B978-0-12-394584-6.00015-7.
34) J. K. Oleiwi, M. S. Hamza, M. S. Abed. "A study of the hardness and wear rate of elastomer composites reinforced by Al_2O_3 and SiO_2 particles." Eng. Technol. J. 27, 1423–1434 (2009),doi: 10.30684/etj.27.7.16.
35) K. Tsongas, D. Tzetzis, G. Mansour. "Mechanical and vibration isolation behaviour of acrylonitrile-butadiene rubber/multi-walled carbon nanotube composite machine mounts." Plast. Rubber Compos. 46(9), 458–468 (2017). doi:10.1080/14658011.2017.1391975.
36) L. Shan, C. Y. Tan, X. Shen, S. Ramesh, M. S. Zarei, R. Kolahchi, M. H. Hajmohammad. "The effects of nano-additives on the mechanical, impact, vibration, and buckling/post-buckling properties of composites: A review." J. Mater. Res. Technol. 24, 7570–7598 (2023). doi:10.1016/j.imrt.2023.04.267.
37) B. You, S. Jin. "Preparation of hydrophobic modified silica with Si69 and its reinforcing mechanical properties in natural rubber." Materials 17(13), 3131

(2024). doi:10.3390/ma17133131.

38) A.A. Nayeeif, M.A. Abdulrazzaq, and H.A.K. Ali, "Dynamic response study of the vibration of a washer," AIP Conf. Proc., 2787 (1) 090036 (2023). doi:10.1063/5.0149158.

39) M. A. Mansour, A. B. Ibrahim, and K. S. Ahmed, "Surface Treatment Effects on the Mechanical Properties of Silica Carbon Black Reinforced Natural Rubber/Butadiene Rubber Composites," Polymers, vol. 16, no. 4, p. 512, Feb. 2024. doi: 10.3390/polym16040512.4

40) Z. Zhao, W. Meng, B. Yan, G. Qiao, Y. Qin, Y. Wang, T. Yang, H. Ren. "Mechanical constitutive model of stand-off damping composites layered rubber core under wide strain rates." Sci. Rep. 15, 10516 (2025). doi:10.1038/s41598-025-10516.

41) H. A. K. Ali, M. S. Abed, A. A. Nayeeif. "Response of viscous damping of dashpot containing hybrid nanofluid." J. Adv. Res. Fluid Mech. Therm. Sci. 67(1), 52–65 (2020). doi:10.37934/arfmts.67.1.5265.

42) A. K. Nayeeli, H. A. K. Ali, and M. F. Farhan, "Structural vibration effect of digital controlled CNC machines on the precision of laser work," AIP Conf. Proc., 2415 (1) 060003 (2022). doi:10.1063/5.0092672.